INL/EXT-13-29896

ATRC Neutron Detector Testing Quick Look Report

T. C. Unruh
B. M. Chase
J. L. Rempe

August 2013

The INL is a U.S. Department of Energy National Laboratory
operated by Battelle Energy Alliance

INL/EXT-13-29896

ATRC Neutron Detector Testing Quick Look Report

T. C. Unruh
B.M. Chase
J. L. Rempe

August 2013

Idaho National Laboratory
Idaho Falls, Idaho 83415

http://www.inl.gov

Prepared for the
U.S. Department of Energy
Office of Nuclear Energy
Under DOE Idaho Operations Office
Contract DE-AC07-05ID14517

CONTENTS

FIGURES

TABLES

1. INTRODUCTION

As part of the Advanced Test Reactor (ATR) National Scientific User Facility (NSUF) program, a joint Idaho State University (ISU) / French Alternative Energies and Atomic Energy Commission (CEA) / Idaho National Laboratory (INL) project was initiated in FY-10 to investigate the feasibility of using neutron sensors to provide online measurements of the neutron flux and fission reaction rate in the ATR Critical Facility (ATRC). A second objective was to provide initial neutron spectrum and flux distribution information for physics modeling and code validation using neutron activation based techniques in ATRC as well as ATR during depressurized operations. Detailed activation spectrometry measurements were made in the flux traps and in selected fuel elements, along with standard fission rate distribution measurements at selected core locations. These measurements provide additional calibration data for the real-time sensors of interest as well as provide benchmark neutronics data that will be useful for the ATR Life Extension Program (LEP) Computational Methods and V&V Upgrade project. As part of this effort, techniques developed by Prof. George Imel will be applied by Idaho State University (ISU) for assessing the performance of various flux detectors to develop detailed procedures for initial and follow-on calibrations of these sensors. In addition to comparing data obtained from each type of detector, calculations will be performed to assess the performance of and reduce uncertainties in flux detection sensors and compare data obtained from these sensors with existing integral methods employed at the ATRC.

The neutron detectors required for this project were provided to team participants at no cost. Activation detectors (foils and wires) from an existing, well-characterized INL inventory were employed. Furthermore, as part of an on-going ATR NSUF international cooperation, the CEA sent INL three miniature fission chambers (one for detecting fast flux and two for detecting thermal flux) with associated electronics for assessment. In addition, Prof. Imel, ISU, has access to an inventory of Self-Powered Neutron Detectors (SPNDs) with a range of response times as well as Back-to-Back (BTB) fission chambers from prior research he conducted at the Transient REActor Test Facility (TREAT) facility and Neutron RADiography (NRAD) reactors. Finally, SPNDs from the National Atomic Energy Commission of Argentina (CNEA) were provided in connection with the INL effort to upgrade ATR computational methods and V&V protocols that are underway as part of the ATR LEP.

Work during fiscal year 2010 (FY10) focussed on design and construction of Experiment Guide Tubes (EGTs) for positioning the flux detectors in the ATRC N-16 locations as well as obtaining ATRC staff concurrence for the detector evaluations. Initial evaluations with CEA researchers were also started in FY10 but were cut short due to reactor reliability issues. Reactor availability issues caused experimental work to be delayed during FY11/12. In FY13, work resumed; and evaluations were completed.

The objective of this "Quick Look" report is to summarize experimental activities performed from April 4, 2013 through May 16, 2013. This report documents the data and observations obtained while completing these activities, allowing ISU and other interested organizations, such as CEA, the opportunity to evaluate the performance of detectors included in this program. Previous work and documentation related to testing are discussed in Section 2. The observations for the most recent testing campaign are described in Section 3. Conclusions, recommendations, and proposed future work are summarized in Section 4. References are listed in Section 5.

2. BACKGROUND

Understanding neutron flux in a nuclear reactor is critical for safe operation of the reactor as well as for evaluating experiments in MTRs. Recently, it has become increasingly clear that further research into real-time flux sensors are needed to evaluate operating conditions as well as fuels and materials tests in ATR. Several activities were planned to research real-time detectors. As documented in Reference 1 and 2 (see Table 1), four specific activities were envisioned to be completed in this project. Each activity has 3 experimental configurations associated with the detector evaluations (see Figure 1). All of these activities were completed except Activity 4B. It is anticipated that Activity 4B will be completed at the end of FY-13.

Table 1. Summary Description of the Planned Experimental Activities.

Activity	Description
I	A. Install and perform mechanical tests of Experiment Guide Tube (EGT) positioning devices for the N-16 positions with the ATRC in a shutdown configuration. B. Experimentally evaluate potential radiation hazards to personnel due to neutron streaming to the surface of the ATRC water tank up the EGT assemblies. This is done via a series of low-power ATRC runs with the guide tube assemblies and dry tubes installed, but without instrumentation in place.
II	A. Perform NW Flux Trap activation foil and wire irradiations for each of three critical shim positions at 600 watts, beginning with the balanced configuration. B. Perform core flux wire irradiation with U/AL and Cu/Au wires for the balanced critical shim position at 600 watts.
III	Test SPND detectors in the ATRC N-16 guide tubes in the positions of interest shown in Figure 1, with three different critical configurations of the outer shim cylinders. For each configuration, ascend to 600 watts with at least four intermediate power levels beginning at approximately 1 milliwatt. With each configuration at the maximum power, measure the axial flux profiles in the 6 N-16 locations shown in Figure 1.
IV	A. Test SPND and fission chamber detectors in the ATRC N-16 guide tubes in the positions of interest shown in Figure 1, with three different critical configurations of the outer shim cylinders. For each configuration, ascend to 600 watts with at least four intermediate power levels beginning at approximately 1 milliwatt. With each configuration at the maximum power, measure the axial flux profiles in the locations shown in Figure 1. B. Test the BTB fission chambers in the NW IPT. For this test, there may be multiple runs, to accommodate tests with a co-located fast fission chamber, a collocated thermal fission chamber, and with co-located fast and thermal fission chambers. During each run, SPNDs will be positioned in the N-16 positions to monitor power.

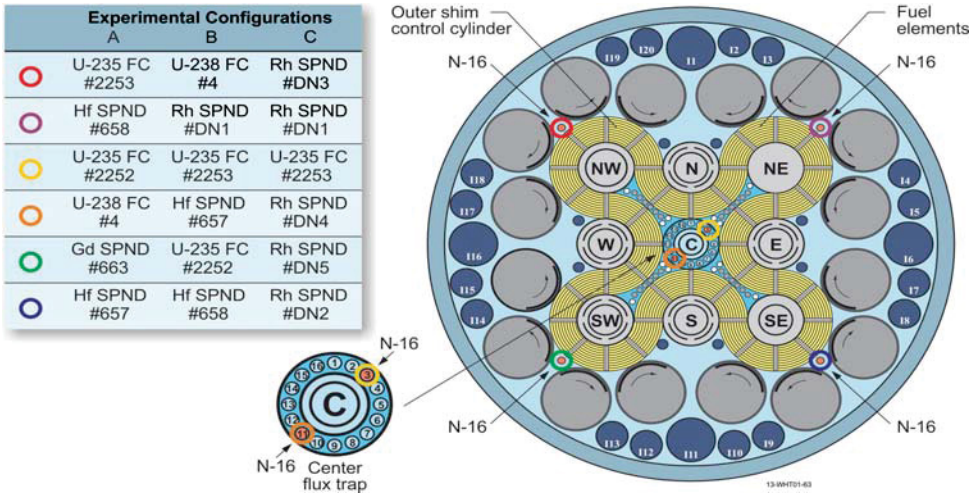

Figure 1. ATRC In-core Sensor Locations

2.1. Previous Work and Supporting Documentation

Initial work performed in FY-10 included Activity 1A/1B. Activity 3B was started, but not completed due to reactor reliability issues. Activity 1A was completed in TP-2-10, "N-16 Experiment Guide Tube Mock-up fitment in ATRC."[5] Activity 1B was completed, and activity 3B was started in TP-4-10, "N-16 Experiment Guide Tube Testing."[4]

Activity 2A/2B was performed under test plan TP-3-10, "Flux Runs for Activation Foil Measurements"[6] and test plan TP-3-12, "Activation Foil Measurements - Irradiation 5"[7] with results detailed in INL/EXT-10-19940 and INL/EXT-11-23348, "Advanced Test Reactor Core Modeling Update Project Annual Report for Fiscal Year 2010"[8] and "Advanced Test Reactor Core Modeling Update Project Annual Report for Fiscal Year 2011."[9]

In addition, previous work of interest for validation purposes includes the flux run 12-8 for core loading 12-13 performed in TP-4-12, "SE-192 Reactivity and Axial Flux Measurement"[10] with results detailed in ECAR-2089, "RML Data Package Flux Run 12-8 TP-4-12"[11]. This test plan was performed for the Bettis SE-192 experiment and was the last core configuration prior to starting TP-2-13 that was used for these in-core sensor evaluations. Hence, it is the most applicable flux measurements with the only minor exception being that the N-16 mock-ups are removed and the EGTs/dry tubes/detectors are in their place. However, it should be noted that the core loadings don't match exactly due to a typo in the TP-4-12 test plan for the H-position irradiation facilities. The H-position irradiation loadings listed in TP-2-13 are correct, and the same for TP-4-12.

2.2. Test Plan Details

An ATRC test plan governs the operation of ATRC and must be written to meet the experimental objectives. The test plan describes the ATRC Facility core changes and operations to be performed to test in-core neutron detectors in 6 Experiment Guide Tube (EGT) assemblies in the 4 inner lobe and 2 Center Flux Trap (CFT) N-16 locations. As outlined in Table 2, the first test will insert the in-core neutron detectors to test signal response at various power levels up to 600 watts and test the vertical movement of the EGT/dry tube/detector assemblies at 600 watts. The second test will evaluate the in-core detectors at various power levels up to 600 watts with the in-core detectors at core mid-plane and then measure the axial flux profile of the core at 600 watts. The third test will place the in-core detectors at core mid-plane and measure the power split for 3 outer shim configurations, balanced, un-balanced toward NW, and un-balanced away from NW. The fourth, fifth and sixth tests will remove the installed in-core neutron detectors and insert different in-core neutron detectors that are capable of measuring fast and thermal neutron fluxes. The fourth test will repeat the tests performed in tests 1, 2, and 3 as well as perform a measurement of the ratio between the response for the thermal in-core detector and the fast in-core detector for a balanced Outer Shim Control Cylinder (OSCC) configuration. The fifth test will repeat the tests performed in tests 2 and 3 as well as perform a measurement of the ratio between the response for the thermal in-core detector and the fast in-core detector for an unbalanced core toward the northwest lobe OSCC configuration. The sixth test will repeat the tests performed in tests 2 and 3 as well as perform a measurement of the ratio between the response for the thermal in-core detector and the fast in-core detector for an unbalanced core away from the northwest lobe OSCC configuration. The seventh, eighth and ninth tests will repeat the tests performed in tests 1, 2, and 3 with different in-core detectors. Test objectives from the test plan are detailed

in Table 2.

Table 2. Test Plan TP-2-13 Details

Activity	Experimental Configuration	Test	Description/Objective
III	A	1) Detector checkout	Verify detector response to neutrons and set fission chamber voltages
III	A	2) Power linearity tests	Verify detector response to power levels
III	A	2) Axial flux profile setup	Measure axial flux profile to determine location for maximum flux
III	A	2) Axial flux profile measurement	Measure axial flux profile
IV-A	A	3) Reactor power split measurements	Measure detector response when OSCCs are: 1) balanced, 2)with the NW OSCCs +4 from balanced position, and 3) with the NW OSCCs -4 from balanced position
IV-A	B	4) Detector checkout	Verify detector response to neutrons
IV-A	B	5)Power linearity tests	Verify detector response to power levels when OSCCs are: 1) balanced, 2)with the NW OSCCs +4 from balanced position, and 3) with the NW OSCCs -4 from balanced position
IV-A	B	6) Axial flux profile measurement with power split	Measure axial flux profile when OSCCs are: 1) balanced, 2)with the NW OSCCs +4 from balanced position, and 3) with the NW OSCCs -4 from balanced position
III	C	7) Detector checkout	Verify detector response to neutrons
III	C	8) Power linearity tests	Verify detector response to power levels
III	C	8) Axial flux profile measurement	Measure axial flux profile
IV-A	C	9) Reactor power split measurements	Measure detector response when OSCCs are: 1) balanced, 2)with the NW OSCCs +4 from balanced position, and 3) with the NW OSCCs -4 from balanced position

2.3. Experimental Details

Several types of neutron detectors were evaluated to understand the operational characteristics needed for use in ATRC and for ATR experiments. Details related to the design, operation and evaluation of each type of sensor is discussed in the following sections.

2.3.1. Fission Chambers

Fission chambers, which are ion chambers with a fissionable material deposit on the inner wall, offer a method for real-time flux measurement (see Figure 2). The fission fragments provide a very large pulse from the neutron-induced reaction and can be used in either pulse or direct current mode. Normally highly-enriched ^{235}U is used for the coating, which makes them sensitive to thermal neutrons. However, other deposits can be used, such as ^{238}U, ^{242}Pu, or ^{232}Th, providing a higher neutron energy cutoff.

Characteristics of the miniature fission chambers included in the ATRC evaluations are listed in Table 3. Miniature fission chambers are used in pulse mode using current preamplifier electronics. Uranium coat-

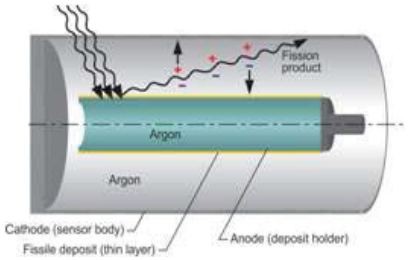

Figure 2. Fission Chamber

ing masses were chosen in order to provide a high fission rate in ATRC flux (from 10^3 to 10^5 cps). To protect these fission chambers and to preclude any leakage from fission chamber components into the ATRC coolant, chambers were placed in tinted Lucite tubes.

2.3.2. SPNDs

SPNDs have been used effectively as in-core flux monitors for decades in commercial nuclear power reactors and materials testing reactors world-wide. SPNDs rely on interactions of neutrons and atomic nuclei to produce a current which is proportional to the neutron flux.

A typical SPND consists of a coaxial cable containing an inner electrode (the emitter), which is surrounded by insulation and an outer electrode (the collector). In an "integral SPND," the lead cable and detector are mated directly to each other; the insulation of both sections are identical; and the collector of the detector section is also the outer sheath of the lead cable section (see Figure 3). Modular SPND assemblies are made from separate detector and lead cable sections. Typically, SPND characteristics of interest include size, material compatibility at high temperatures, sensitivity, response time, and burn-up rate.

Characteristics of SPNDs evaluated in this project are listed in Table 3. SPNDs were also placed in tinted Lucite tubes to prevent any unwanted leakage of component materials (if they are not leak-tight) and to reduce unwanted noise from the SPND cables being in contact with metal surfaces. SPNDs were inserted into the ATRC N-16 positions using the EGTs.

2.3.3. Flux Wires and Foils

While not evaluated during the time period covered in this quick look report, testing flux wires and foils provide validation data to determine the neutron flux and neutron spectrum used during evaluations. An example of the various flux wires and foils with the accompanying test hardware is shown in Figure 4.

Table 3. In-core Neutron Detector Characteristics Under Evaluation

Detector	**Composition, Geometry, and Mass**				
CEA Miniature Fission Chambers	Fissile Deposit	Anode/Fill Gas	Cathode / Fill Gas	Extension Cable	Maximum Core Insertion Mass
Miniature Thermal Fission Chamber	Mass 30µg (deposit on anode) U-235 98.5 % U-234 0.063% U-236 0.038% U-238 1.409%	Material: SS304L (impurities of Co 0.02%) ID: 1.6 mm OD: 2 mm Length: 14 mm Fill Gas: Argon+ 4% N_2 Pressure : 5 bars	Material: SS347(impurities of Co 0.2%) ID: 2.5 mm OD: 3 mm Length: 33 mm except cable Fill Gas: Argon+ 4% N_2	Mineral cable (1CCAc22Si50 Ohms) OD: 2.2 mm Length: 10 mm Materials Sheath: SS304L Insulation: SiO2 (>99.5%) Wires: Copper (impurities of Zirconium 0.19%) Shield: Copper	Detector: U-235: 30 µg SS304: < 2g Fill Gas: < 5E-4 g Extension Cable: SS304: < 300 g SiO_2 : < 12 g Cu : < 8 g
Miniature Fast Fission Chamber	Mass: 1000 µg (deposit on cathode) U-238 : 99.964% U-235 : 0.0354% U-234 : 0.0003%	Material: SS316L ID : / OD: 1 mm Length: 51.5 mm Fill Gas: Argon Pressure: 9 bars	Material: SS316L ID: 6.3 mm OD: 8 mm Length: 33.5 mm Fill Gas: Argon Pressure: 9 bars	Organic cable RG58BU OD: 6.15 mm ; length 10 m Materials Sheath: PVC Insulation: polyethylene (PE) Wires: copper clad steel (CCS)	Detector: U-235 : 30 µg SS316L : <5 g Fill Gas: 1E-2 g Extension Cable: SS304: 0 g PVC : < 30 g PE : < 15 g Wires: < 3 g
SPNDs	Emitter	Lead Wire(s)	Insulation	Sheath (Collector)	Maximum Core Insertion Mass
Hafnium Manufacturer: B&W Fuel Sensitivity 4.7e-21 A/nv (vendor specified)	Hafnium (minimum 97.5% with up to 2.5% Zr) – fast response Diameter: 0.4572 mm Length: ~ 400 mm (coiled to reduce length) Mass: 0.873 g (nominal)	Number: Two Material: Inconel 600 Diameter: 0.203 mm	Al_2O_3 Purity: 99.65% Compaction: ~70%	Inconel 600 ID: 0.904 mm OD: 1.372 mm	Hafnium: 0.897 g Inconel 600: 9.02 g Al_2O_3: 0.82 g
Gadolinium Manufacturer: B&W Fuel Sensitivity 5.0e-22A/nv (vendor specified)	Gadolinium (99.7%) – fast response Diameter: 0.559 mm Length: ~25 mm Mass: 0.0508 g	Number: Two Material: Inconel 600 Diameter: 0.229 mm	Al_2O_3 Purity: 99.65% Compaction: ~70% ID: 0.559	Inconel 600 ID: 1.017 mm OD: 1.575mm	Gadolinium: 0.055 g Inconel 600: 12.50 g Al_2O_3: 2.29 g
Rhodium	Rhodium Diameter – 1 mm Length – 20 mm	Cu	Acrylic ID: 1.0 mm OD: 1.5 mm Length: 20 mm	SS-304 ID: 1.5 mm OD: 1.9 mm Length: 100 mm	Rhodium: 1g SS:0.5 g
Flux Wires	Materials	Diameter	Maximum Length		Maxium Core Insertion mass
	U_{235}-Aluminum	1 mm	0.635 cm		
	Copper-1.55 Gold	1 mm	1.27 cm		10 grams

Table 3. In-core Neutron Detector Characteristics Under Evaluation

Detector	**Composition, Geometry, and Mass**				
Foils	Material	Encapsulation Material	Maximum Thickness (mm)	Maximum Diameter	Maximum Core Insertion Mass
Thermal-neutron Detection	Gold (100 %)	None	0.0127	1 cm	200 mg
	Manganese-Copper (80%/20%)		0.0127	1 cm	100 mg
Epithermal-neutron Detection	Indium (> 99%)	Cadmium Covers	0.0127	1 cm	200 mg
	Gold (> 99%)				
	Tungsten (>99%)				
	Cobalt (>99%)				
	Manganese-Copper (80%/20%)				
	Copper (>99%)				400 mg
	Scandium (>99%)				200 mg
Fast-neutron Detection	Niobium (>99%)	Boron Sphere	0.0127	2.54 cm	1 gram
	Rhodium (>99%)				
	Indium (>99%)				
	Titanium (>99%)				
	Zinc (>99%)				
	Nickel (>99%)				
	Iron (>99%)				
	Copper (>99%)				
Foil Encapsulation	Material	Application	Thickness, mm	Diameter	Mass
	Cadmium (> 99%)	Epithermal-neutron Detection	1	1.27 cm	1 g
	Boron Sphere (>99%)	Fast-neutron Detection		2.54 cm OD 1.27 cm ID	115g

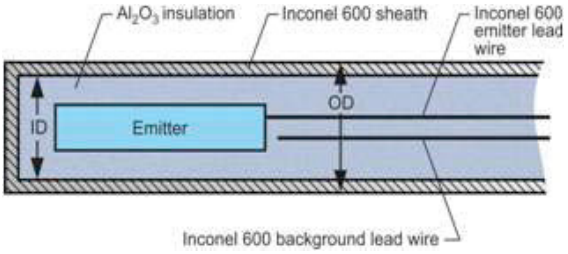

Figure 3. SPNDs

Figure 4. Flux Wires and Foils

A summary of the advantages and disadvantages of each type of in-core sensor is listed in Table 4.

Table 4. Standard In-core Neutron Detector Characteristics

Option	Advantages	Disadvantages
Foils/ Wires	• Inexpensive • Small • Accurate	• Only detect thermal or fast fluence • Requires post-irradiation analyses • Not real time • Only integral measurement
SPNDs	• Real time • No power supply needed • Simple and robust structure • Small diameter • Good stability at high temperatures and pressures • Generate reproducible linear signal	• Require calibration • Only detect thermal flux • Response time /lifetime/sensitivity tradeoff considerations • Background discrimination required
Miniature Fission Chambers	• Real time • Thermal or fast neutron flux monitoring, depending on deposited fissile material • Small diameter • Reproducible linear signal	• Only fast or thermal flux • Require calibration • Require power supply • High temperature survivability • High pressure fill gas • Lifetime /sensitivity/flux tradeoff considerations • Gamma discrimination required

2.3.4. Experimental hardware

In-core sensors were inserted into the ATRC in N-16 positions using Experiment Guide Tubes (EGTs). The EGTs are primarily fabricated from aluminum to minimize their weight. However, selected components, such as the guide tube shown in Figure 5 are made from stainless steel 304 for additional robustness. As illustrated in Figure 5, the six EGTs mechanically position detectors at a specified vertical location in the four N-16 exterior positions and two Center Flux Trap N-16 positions. The EGTs were supported above the reactor by attaching to the reactor control bridge.

The position control and detector response are controlled and measured via LabView software to allow all sensors to either individually or simultaneously move and measure the local neutron flux and provide a three-dimensional measurement of the overall neutron flux.

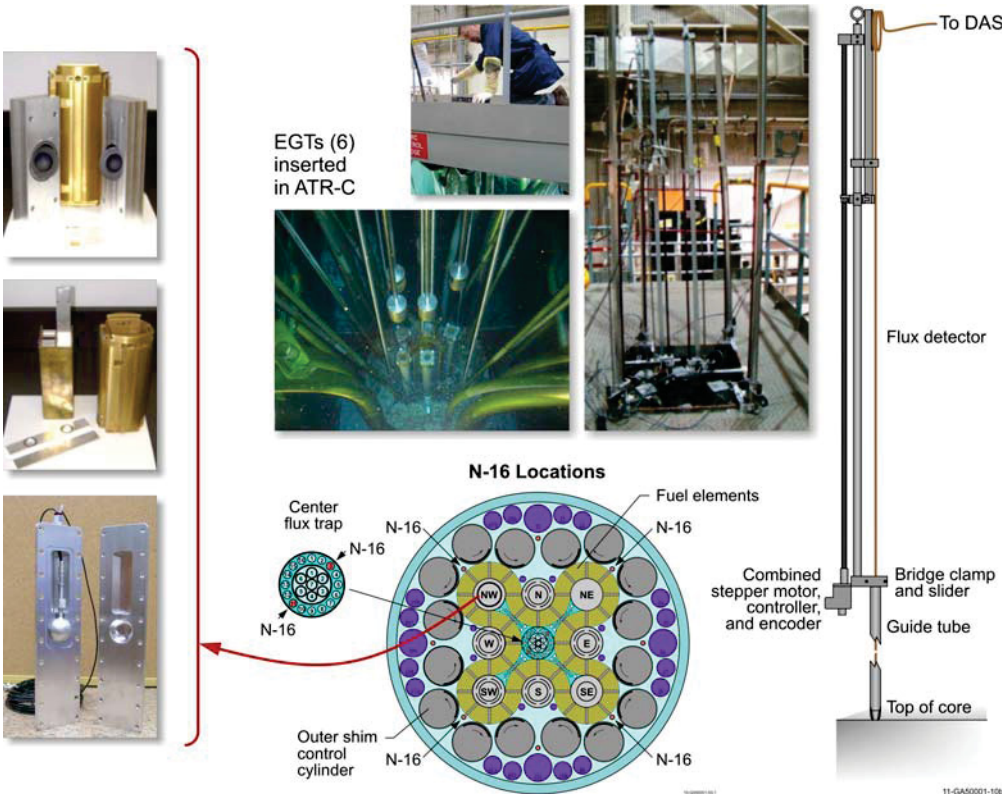

Figure 5. EGTs in ATRC

3. EXPERIMENTAL OBSERVATIONS

Detector evaluations were performed for a variety of operational conditions. As previously discussed, the reactor was brought to specified power levels between 0.01W and 600W. In addition, measurements were taken with the reactor shut down prior to startup and with the reactor shut down after startup. In order to assess if the detectors could be used to monitor various power splits, the reactor was purposely operated in an unbalanced condition, meaning the OSCCs in the NW lobe were positioned at +/-4 degrees from their nominal critical position. The following sections summarize the initial observations from experimental data collection and initial analysis.

3.1. Testing

As noted previously, the purpose of this project was to gain a more complete understanding of in-core sensor performance in a nuclear reactor. The response of various sensors were compared in numerous operational conditions to determine their usefulness for reactor operations and reactor experiments. Initially, the sensors were verified to be operational, then the detectors were used to track reactor power. Typical data obtained from power level testing in test 8 is shown in Figure 6.

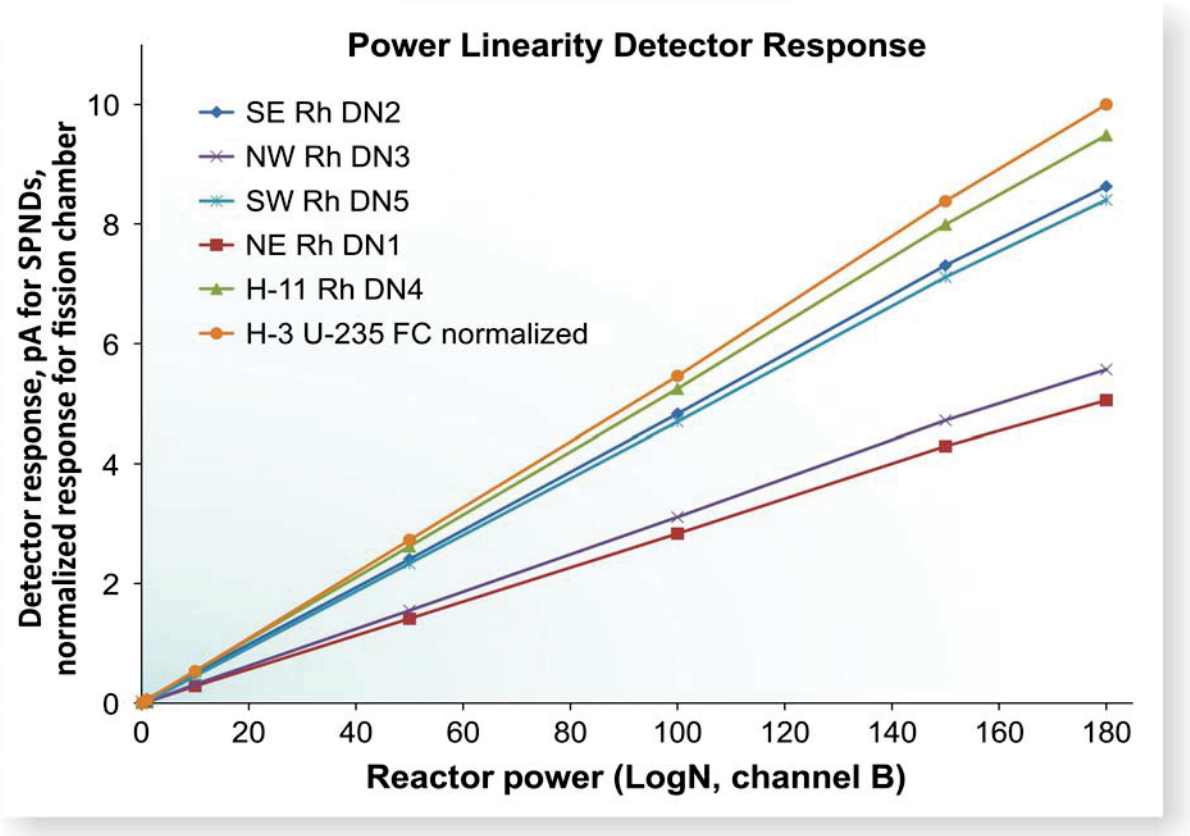

Figure 6. Comparison of Power Measurements Obtained from Rhodium SPNDs and a Fission Chamber from Activity III, Test 8, Experimental Configuration C

Further testing continued by measuring the axial flux profile across the full length of travel of the EGTs. The position started outside the core above the reactor and contiued until the EGTs reached the lower limit touching the bottom reactor support plate. The transition between the active region of the core top and bottom of the core seems to be the most pronounced in the center flux trap positions, H-3 and H-11. Representative data obtained from axial flux testing from test 8 is shown in Figure 7.

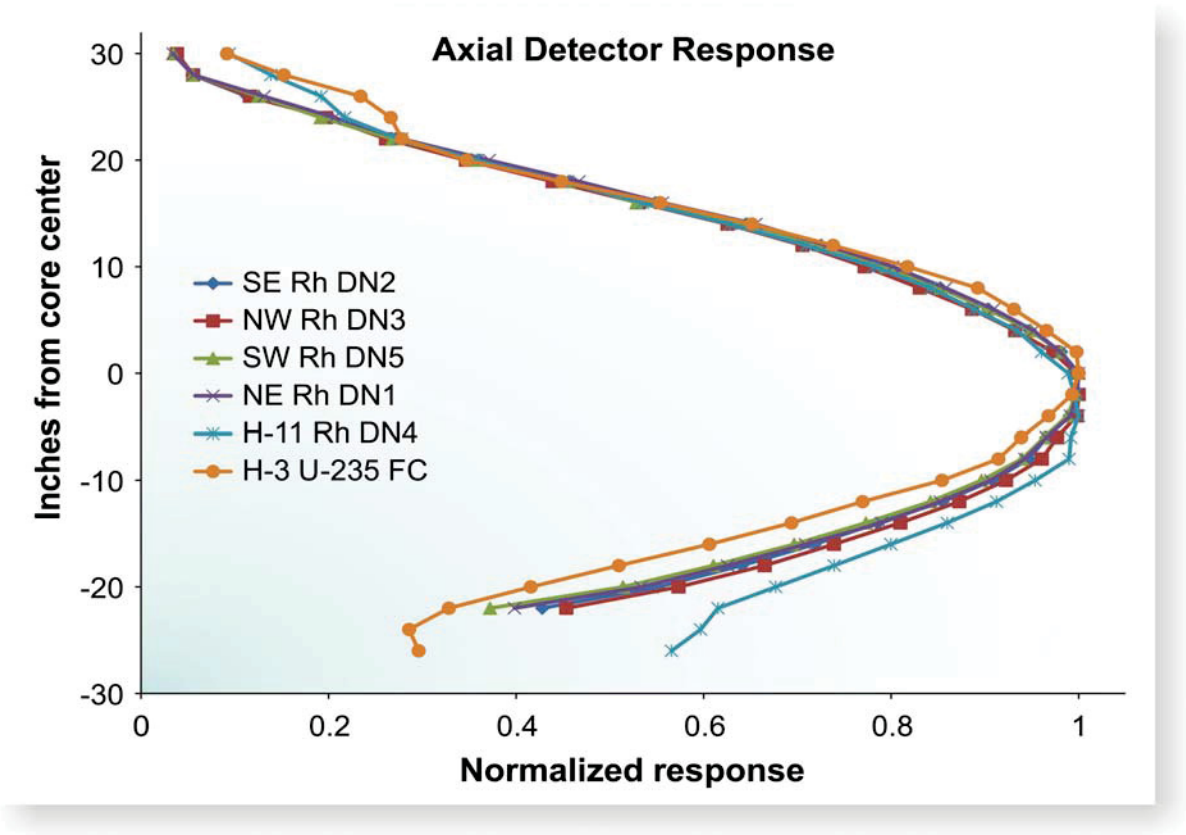

Figure 7. Axial Flux Profile from Rhodium SPNDs and a Fission Chamber from Activity III, Test 8, Experimental Configuration C

In addition to data collection, various insights were gained during the testing of the in-core sensors related to installation, operation, and data analysis and are summarized in the following sections.

3.1.1. Signal Response

Each type of detector demonstrated unique signal responses. The SPNDs displayed a current from -0.04 to 6 pico-amps. Due to the half-lives of the emitter materials, each type of SPND demonstrated a different response time for the signal to stabilize. Similarly, the decay of each type of emitter required careful consideration when monitoring power drops or recoveries from a reactor shutdown. This phenomenon can be seen on Figure 8 when the reactor was shut down during the middle of testing and the Hf-657, Hf-658,and Gd-663 signals did not return to the same values prior to shutdown.

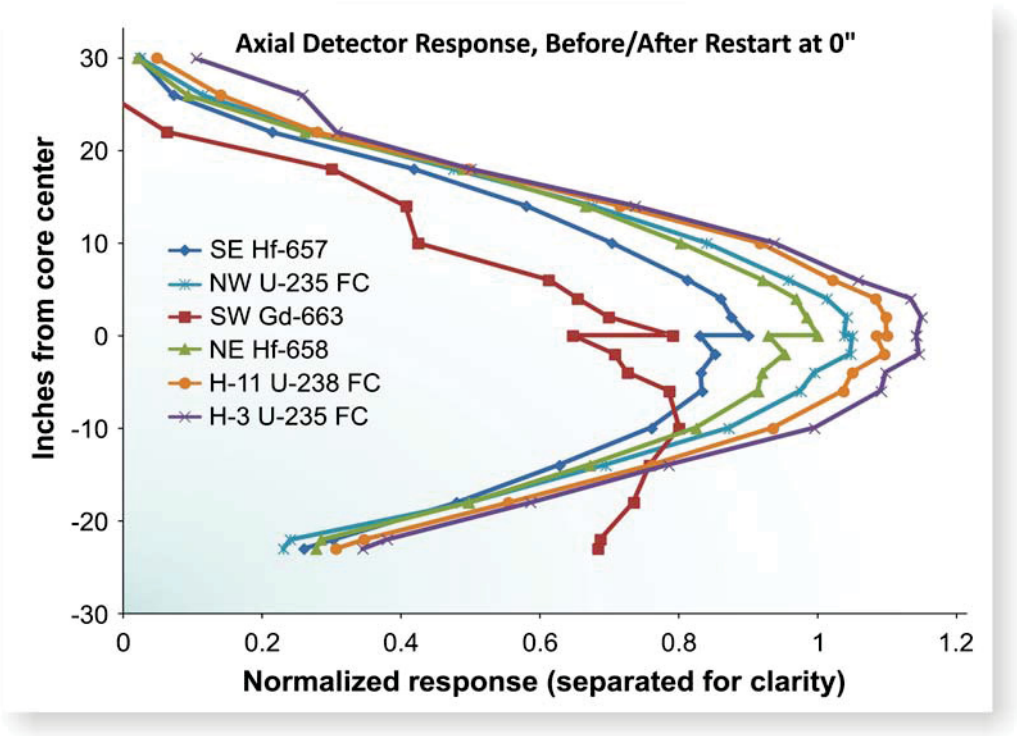

Figure 8. Axial Flux Profile from Rhodium SPNDs and a Fission Chamber, Before and After a Reactor Restart with the EGTs Located at Core Centerline from Activity III, Test 2, Experimental Configuration A

The fission chambers displayed electrical pulses that corresponded to count rates from 0 to $4x10^6$ counts per second (cps). Unlike the response from the SPNDs, the response from the fission chambers did not have delays built into their signals. In addition, the fission chambers responded instantaneously to reactor power changes. As shown in Figure 8, the fission chamber signals returned to essentially the same value prior to a shutdown, whereas the SPND signals varied.

3.1.2. Power Level Linearity

The detector responses were checked at reactor instrument Log-N channel B readings of 0.00065 (shut down) 0.02, 0.1, 1, 10, 50, 50, 100, 150 and 180 (approximately 600 W). As shown in Figure 6, all the detectors demonstrated a linear response to reactor power changes; but depending on core location, the slopes differed between the detectors in the north, south and center locations. This phenomenon was observed in all detectors. Hence, it is suspected that power in various core locations varies linearly with reactor power, but not equally with reactor power.

3.1.3. Detector Failures

One of the SPNDs and one of the fission chambers experienced failure during testing. Both failures were due to water egress in the dry tubes, eventually shorting the detectors that were not constructed to be leak-tight. The wet Rh SPNDs displayed a signal in the micro-amp range, which is several orders of magnitude higher than the upper value of its typical range (pico-amps). The fission chamber displayed random

noise pulses. CEA has indicated that a thorough drying of the fission chamber and cabling would likely return the fission chamber to its previous operational condition. It is suspected the SPND would similarly benefit from a through drying. However, the detectors could not be thoroughly dried and retested in this series of experiments

3.1.4. Measurement Repeatability

As previously discussed in 3.1.1 and 3.1.2, the measurement repeatability was very consistent for the fission chambers during all testing conditions and irradiation history. Due to the inherent manner in which SPNDs operate, the consistency of the measurements was closely related to their irradiation exposure. SPND response at the beginning of testing was not consistent with their response at the end of testing due to the increasing activation of the emitter during irradiation and decay of the emitter if the reactor is shut down during testing. SPND signal buildup during irradiation must be considered.

3.1.5. Sensitivity Comparisons

Detailed flux measurements using foils and wires in the N-16 positions have not been taken, so absolute sensitivities can not be determined. However, sensitivity comparisons between detectors can be determined by estimating the flux in the N-16 positions and by using cross-comparisons for each detector position.

4. CONCLUSION

Various real-time in-core flux sensors have been evaluated at the ATRC as part of a joint ISU/INL/CEA project funded through the ATR NSUF. The sensors were evaluated a various reactor power levels and at different positions throughout the core. The sensors were used to measure reactor lobe power as well as axial flux. Both fast and thermal neutron flux measurements were taken for comparison.These evaluations complete the ISU/INL/CEA project. However the new capabilities developed from this project are available for future testing and evaluations of in-core sensors.

4.1. Experimental Setup and Testing

During sensor evaluations, it was noted that several areas of operation could be improved upon in future testing. Most notably is that the dry tubes remain dry throughout testing. The dry tubes were initially inserted into the ATRC canal in 2010, so it is unknown when the water leaked into the tube in the NW N-16 position. The Labview program developed for this project should be updated to allow for all drives to be moved simultaneously and to log data when requested.

Interfacing detector response with the reactor log count rate detectors would also aid in evaluations to verify the neutron flux remains constant throughout testing.

4.1.1. Tests Requiring Further Evaluation

The schedule to complete testing in the ATRC did not allow for appropriate drying of the fission chamber, so water ingress into the dry tube prevented further testing with the U-238 fission chamber. Further comparisons between thermal and fast flux would aid in understanding detector response between each type of detector.

Flux wire and foil measurements in the N-16 positions would be beneficial for comparisons between the real-time sensors and integral measurements.

4.2. Future Work

It is expected that in-core sensor evaluations will continue in the ATRC. The size and flexibility of the ATRC reactor core allows for alternative and advanced in-core sensors to be tested in a variety of conditions. Planned tests for future ATRC tesing are identified in this section.

4.2.1. Back-to-Back (BTB) Fission chamber

BTB fission chambers, which are often called 2π fission chambers because they are designed to count almost all fission fragments emitting from a thin deposit in a 2π solid angle, provide the most accurate measure of fission reaction rates. For the ATRC evaluations, BTB chambers, developed in the Zero Power Physics Reactor (ZPPR) programs will be used. The BTB fission chambers are bisected hollow aluminum spheres, with stainless steel collector plates attached to the inside spherical surface of each half of the detector. Two stainless steel foils, coated with uranium, plutonium, or neptunium, were positioned such

that the uncoated sides are in contact. These foils act as the center divider inside the BTB chamber volume, and are kept at the same electrical potential. Each spherical half has its own purge gas (P-10, a mixture of argon and methane) supply and exhaust lines and coaxial cable signal leads.

The counting gas continuously flows through these fission chambers. This allows a chamber to be built that can be easily opened and allow fissile material deposits to be changed. There are two uses for this capability: first, one can cross-calibrate an unknown fissile material deposit to a known fissile material deposit; and second, reaction rate ratios such as spectral indices, are very accurate because the measurements of BTB fissile material deposits are made at precisely the same time. The disadvantage of this type of chamber is that it is limited in the amount of miniaturization possible. It is necessary to register all of the energy deposited by the fission fragments in order to ensure a full spectrum; and at atmospheric pressure, this range is relatively long. This requires a certain volume in the counting gas, which translates into a minimum fission chamber radius.

Initially, these BTB fission chambers were used for calibration of other detectors at ISU. However, specialized fixtures have been fabricated (see Figure 9) to allow a BTB fission chamber to be inserted into the ATRC NW LIPT alongside a CEA fission chamber to compare their response in near-identical flux conditions. The layout of the test fixture used to insert these BTB fission chambers into the ATRC is shown in Figure 10. Not shown is an additional insert for three in-core sensors to assess the flux gradient across the LIPT that can be used in place of the BTB fission chambers.

Figure 9. Fabricated Back-to-Back Fission Chamber Fixtures

The experimental hardware and procedures developed for this project will be available to other research programs needing to evaluate in-core sensors. Such sensors include Micro-Pocket Fission Detectors (MPFDs) for measuring thermal neutron flux, fast neutron flux and temperature simultaneously and Self-Powered Gamma Detectors (SPGDs) for measuring the gamma heating.

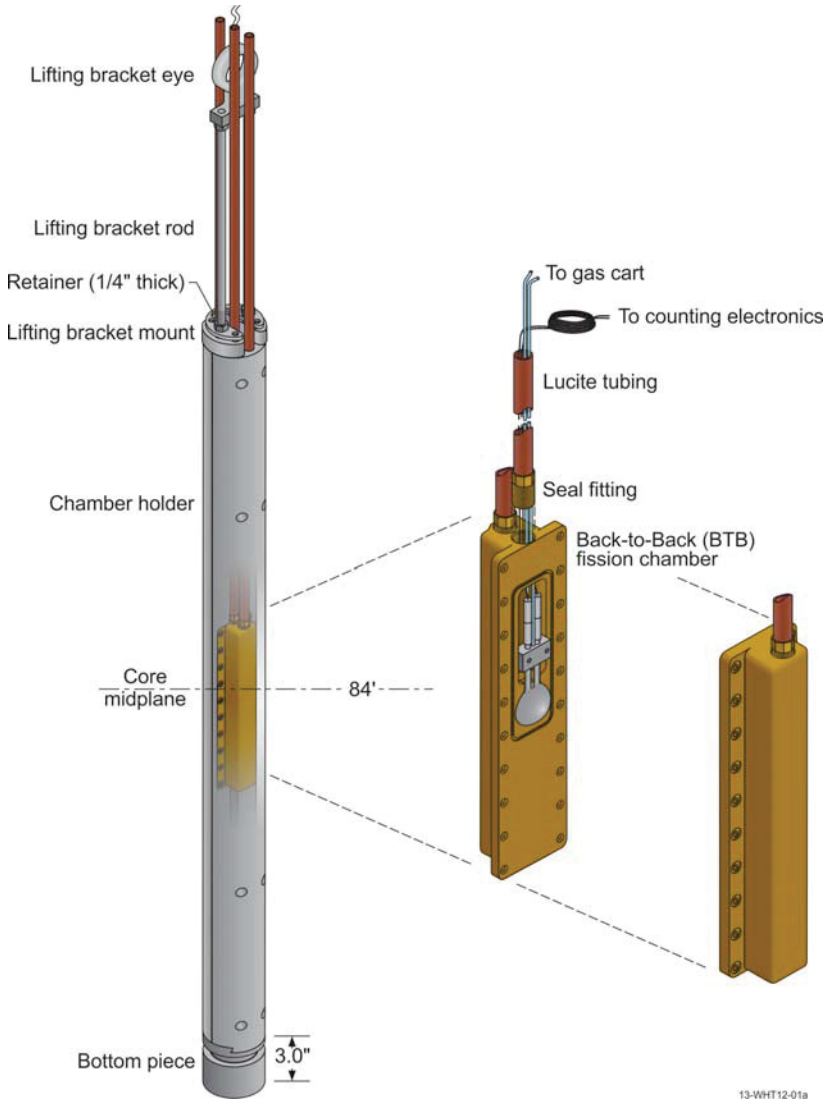

Figure 10. Back-to-Back Fission Chamber Hardware Assembly

4.3. Recommendations

The choice of a real-time in-core flux sensor depends on the end-use requirements. For the purpose of this project, the end-use requirements are based upon the desired experimental measurements in a materials and fuels test or operational information needed to aid in reactor operation.

4.3.1. SPNDs

The simplicity of SPNDs makes them well suited for a variety of measurement conditions. They are small, robust, do not require a power source and generate a steady current while in a thermal neutron field. However, the current response is delayed and requires careful consideration if used to monitor fast power transients. Materials and fuels test are generally only monitoring for anomalies in reactor flux, so the delay

time associated with the use of SPNDs would be acceptable. However if the SPNDs are intended to be used as reactor power monitors, they will need to be supplemented with alternative fast response detectors for input into reactor safety systems. In addition, the SPNDs only operate at higher reactor powers, so they could not be used for the lower neutron fluxes encountered during a reactor startup.

4.3.2. Fission Chambers

The design of fission chambers is inherently more complicated than SPNDs; however, the fast response time associated with their operation can be a benefit for detection of neutron flux. The fission chambers also work well at low neutron fluxes, so it is expected they'd work well to monitor low level reactor power. In addition, very fast power transients would be more easily captured with fission chambers. Also, the fission chambers response does not seem to be heavily dependant on the previous irradiation history of the sensor.

5. REFERENCES

1. J.L. Rempe and D.W. Nigg, FY-10 Irradiation Experiment Plan for the ATR National Scientific User Facility - Idaho State University Project Evaluating Flux, PLN-3351, April 2010

2. D.W. Nigg, J.L. Rempe, and T. Unruh, Qualification of Devices for Neutron Flux Measurements in the Advanced Test Reactor Critical Facility, TEV-885 Revision 1, July 2011.

3. Test Plan, TP-2-13, N-16 Experiment Guide Tube Testing, March 2011.

4. Test Plan, TP-2-10, "N-16 Experiment Guide Tube Mock-up fitment in ATRC, July 2010.

5. Test Plan, TP-4-10, N-16 Experiment Guide Tube Testing, October 2010.

6. Test Plan TP-3-10, Flux Runs for Activation Foil Measurements, November 2010.

7. Test Plan TP-4-13, Activation Foil Measurements – Irradiation 5, August 2013.

8. INL/EXT-10-19940, Advanced Test Reactor Core Modeling Update Project Annual Report for Fiscal Year 2010, September 2010.

9. INL/EXT-11-23348, Advanced Test Reactor Core Modeling Update Project Annual Report for Fiscal Year 2011, September 2011.

10. Test Plan, TP-4-12, SE-192 Reactivity and Axial Flux Measurement, November 2012.

11. ECAR-2089, RML Data Package Flux Run 12-8 TP-4-12, November 2011.

APPENDIX A.

Table A-1. Activity III, Test 2, Experimental Configuration A, Axial Measurements

	Detector Location and Name								
	SE	SE	NW	SW	SW	NE	NE	H-11	H-3
Inches from core center	Hf-657 primary (pico-amps)	Hf-657 background (pico-amps)	U-235 FC 2253 (counts per minute)	Gd-663 primary (pico-amps)	Gd-663 background (pico-amps)	Hf-658 primary (pico-amps)	Hf-658 background (pico-amps)	U-238 FC 4 (counts per minute)	U-235 FC 2252 (counts per minute)
30	0.1439	-0.0838	61036	-0.0650	-0.0867	0.0656	-0.0566	5324	307259
26	0.4675	-0.1409	296890	-0.0372	-0.1561	0.3085	-0.1638	15669	759577
22	1.3934	-0.1255	709507	0.1046	-0.1272	0.8706	-0.0717	31337	905151
18	2.7240	-0.0314	1240520	0.5058	-0.0755	1.6316	0.0483	55931	1474480
14	3.7801	-0.0717	1765730	0.6872	-0.0895	2.2225	-0.0072	80438	2173540
10	4.5847	-0.1540	2193010	0.7163	-0.1640	2.6802	-0.1221	103128	2764740
6	5.2939	-0.0617	2499540	1.0343	-0.0540	3.0755	-0.0020	114894	3120740
4	5.6075	-0.0550	2646060	1.1048	-0.0671	3.2370	-0.0158	121877	3345020
2	5.7068	-0.0376	2721920	1.1803	-0.0639	3.2882	-0.0075	123574	3392620
0	5.8672	0.0560	2711130	1.3370	0.0136	3.3405	0.1273	123752	3369610
0	5.4104	-0.1140	2741930	1.0932	-0.0853	3.1014	-0.0713	122004	3368210
-2	5.5564	-0.0683	2735580	1.1957	-0.0703	3.1821	0.0068	123283	3381450
-4	5.4225	-0.0468	2599660	1.2264	-0.0501	3.0726	0.0077	118119	3238690
-6	5.4334	-0.0121	2547870	1.3284	0.0065	3.0542	0.0926	116666	3219760
-10	4.9580	0.0028	2277110	1.3518	-0.0101	2.7555	0.0921	105234	2936000
-14	4.0922	-0.0129	1813300	1.2801	0.0269	2.2431	0.1225	85751	2317110
-18	3.1248	-0.0095	1294890	1.2417	0.0423	1.6605	0.1826	62314	1728690
-22	1.9649	-0.0156	625701	1.1605	0.0687	0.9483	0.2081	38913	1118540

Table A-2. Activity III, Test 2, Experimental Configuration A, Power Linearity Measurements

	Detector Location and Name								
	SE	SE	NW	SW	SW	NE	NE	H-11	H-3
Power (log N)	Hf-657 primary (pico-amps)	Hf-657 background (pico-amps)	U-235 FC 2253 (counts per minute)	Gd-663 primary (pico-amps)	Gd-663 background (pico-amps)	Hf-658 primary (pico-amps)	Hf-658 background (pico-amps)	U-238 FC 4 (counts per minute)	U-235 FC 2252 (counts per minute)
180	5.8111	0.0774	2744220	1.3939	0.0330	3.3237	0.2016	123829	3375400
150	4.5617	-0.1510	2233710	0.8427	-0.1415	2.5958	-0.1291	102156	2793850
100	3.0939	-0.0477	1458210	0.6682	-0.0687	1.7541	0.0000	66072	1816050
50	1.6411	0.0020	748869	0.3819	-0.0473	0.9098	0.0759	34264	935331

Table A-3. Activity IV-A, Test 3, Experimental Configuration A, Power Split Measurements

	Detector Location and Name								
	SE	SE	NW	SW	SW	NE	NE	H-11	H-3
Estimated Power and Measured Data	Hf-657 primary (pico-amps)	Hf-657 background (pico-amps)	U-235 FC 2253 (counts per minute)	Gd-663 primary (pico-amps)	Gd-663 background (pico-amps)	Hf-658 primary (pico-amps)	Hf-658 background (pico-amps)	U-238 FC 4 (counts per minute)	U-235 FC 2252 (counts per minute)
Balanced Estimated Reactor Power (W)	57.27	57.27	39.75	56.71	56.71	40.53	40.53	55.74	55.74
Balanced Measured Data	5.5394	-0.0578	2672660	1.1862	-0.0571	3.1771	0.0049	117830	3432040
NW OSCC +4 Estimated Reactor Power (W)	56.88	56.88	40.92	56.32	56.32	40.14	40.14	55.74	55.74
NW OSCC +4 Measured Data	5.4784	-0.1058	2980200	1.0785	-0.0877	3.1717	-0.0308	121225	3429890
NW OSCC -4 Estimated Reactor Power (W)	57.67	57.67	38.57	57.11	57.11	40.92	40.92	55.74	55.74
NW OSCC -4 Measured Data	5.7008	-0.0575	2400040	1.1266	-0.0879	3.2621	-0.0231	119408	3401230

Table A-4. Activity IV-A, Test 5, Experimental Configuration B, NW Balanced, Power Linearity Measurements

	Detector Location and Name							
	SE	SE	NW	SW	NE	H-11	H-11	H-3
Power (log N)	Hf-658 primary (pico-amps)	Hf-658 background (pico-amps)	U-238 FC 4 (counts per minute)	U-235 FC 2252 (counts per minute)	Rh DN1 (pico-amps)	Hf-657 primary (pico-amps)	Hf-657 background (pico-amps)	U-235 FC 2253 (counts per minute)
180	5.3917	0.0804	6800	4662350	5.0718	9.9886	-0.1527	2969680
150	4.3334	0.0155	41690	3719020	4.0605	8.1187	-0.1745	2352610
100	2.8983	-0.1686	27923	2458530	2.5646	5.5013	-0.2451	1535630
50	1.5461	-0.0272	14088	1200630	1.5076	3.1037	-0.0352	751567
10	0.3865	-0.0639	2900	228574	0.2602	0.9007	-0.1106	148415

Table A-5. Activity IV-A, Test 5, Experimental Configuration B, NW Unbalanced +4, Power Linearity Measurements

	Detector Location and Name							
	SE	SE	NW	SW	NE	H-11	H-11	H-3
Power (log N)	Hf-658 primary (pico-amps)	Hf-658 background (pico-amps)	U-238 FC 4 (counts per minute)	U-235 FC 2252 (counts per minute)	Rh DN1 (pico-amps)	Hf-657 primary (pico-amps)	Hf-657 background (pico-amps)	U-235 FC 2253 (counts per minute)
180	5.3493	0.0485	-233920	4537990	4.9588	10.0502	-0.1700	3022050
150	4.5038	0.0054	-266840	3754530	4.1994	8.5166	-0.1261	2473880
100	3.0500	0.0140	-264100	2430180	2.8168	5.8436	-0.1083	1609580
50	1.5973	-0.0392	-259930	1201350	1.4253	3.1704	-0.1206	797239
10	0.4137	-0.0535	-268580	241091	0.3005	0.9609	-0.0986	160326

Table A-6. Activity IV-A, Test 5, Experimental Configuration B, NW Unbalanced -4, Power Linearity Measurements

	Detector Location and Name							
	SE	SE	NW	SW	NE	H-11	H-11	H-3
Power (log N)	Hf-658 primary (pico-amps)	Hf-658 background (pico-amps)	U-238 FC 4 (counts per minute)	U-235 FC 2252 (counts per minute)	Rh DN1 (pico-amps)	Hf-657 primary (pico-amps)	Hf-657 background (pico-amps)	U-235 FC 2253 (counts per minute)
180	5.4669	0.0963	5.0463	4593570	5.0986	9.8729	-0.0983	2907890
150	4.6068	0.0576	4.2485	3821780	4.2906	8.3431	-0.0870	2412030
100	3.1442	0.0458	2.8664	2504320	2.9468	5.7825	-0.0685	1573830
50	1.6300	0.0303	1.4437	1226200	1.4684	3.0390	-0.0554	753877
10	0.4417	-0.0034	0.3212	245708	0.3323	0.9187	-0.0233	149808

Table A-7. Activity IV-A, Test 6, Experimental Configuration B, Balanced, Axial Measurements

	Detector Location and Name							
	SE	SE	NW	SW	NE	H-11	H-11	H-3
Inches from core center	Hf-658 primary (pico-amps)	Hf-658 background (pico-amps)	U-238 FC 4 (counts per minute)	U-235 FC 2252 (counts per minute)	Rh DN1 (pico-amps)	Hf-657 primary (pico-amps)	Hf-657 background (pico-amps)	U-235 FC 2253 (counts per minute)
30	0.0502	-0.1253	n/a	79119	-0.0737	0.4674	-0.1155	261902
26	0.4007	-0.1089	n/a	416183	0.4124	1.3035	-0.1204	662979
22	1.1866	0.0277	n/a	1100450	1.0315	3.0560	-0.1166	794495
18	2.3926	-0.0794	23928	1986050	2.1675	4.7900	-0.1501	1325920
14	3.4004	-0.0828	33784	2963910	3.0504	6.7144	-0.1418	1919390
10	4.2996	-0.0727	41398	3739290	3.8952	8.3271	-0.1798	2439150
6	4.9209	-0.0386	50334	4292160	4.5058	9.3326	-0.1880	2831800
2	5.1846	0.0189	39845	4779800	4.8756	9.7293	-0.2248	2927650
0	5.2617	-0.1283	25443	4671240	4.8101	9.7979	-0.2626	2972630
-2	5.3409	0.0544	31812	4638660	5.0606	9.8613	-0.2060	2969220
-6	5.0404	0.0784	11042	4315890	4.8607	9.2607	-0.2409	2816770
-10	4.5349	0.0927	27857	3870250	4.5076	8.2408	-0.2540	2548280
-14	3.7328	-0.0392	23923	3157360	3.6840	6.6268	-0.4186	2100960
-18	2.8470	0.1203	12971	2230930	3.1139	5.0081	-0.2906	1541550
-22	1.7773	0.3242	8113	1011800	2.0594	3.2188	-0.2075	980447

Table A-8. Activity IV-A, Test 6, Experimental Configuration B, NW Unbalanced +4, Axial Measurements

	Detector Location and Name							
	SE	SE	NW	SW	NE	H-11	H-11	H-3
Inches from core center	Hf-658 primary (pico-amps)	Hf-658 background (pico-amps)	U-238 FC 4 (counts per minute)	U-235 FC 2252 (counts per minute)	Rh DN1 (pico-amps)	Hf-657 primary (pico-amps)	Hf-657 background (pico-amps)	U-235 FC 2253 (counts per minute)
30	0.0930	-0.8560	-103710	84130	0.1253	0.5736	-0.0811	271875
26	0.4637	-0.0794	-123340	423905	0.5890	1.4289	-0.1053	695511
22	1.3691	-0.0476	-124970	1071680	1.3329	2.9628	-0.1019	836007
18	2.4173	-0.0683	-123750	1955130	2.2508	4.9243	-0.0809	1339120
14	3.4571	-0.0735	-129640	2859510	3.1908	6.8630	-0.0895	1948470
10	4.3473	-0.0148	-137930	3643680	4.0157	8.4983	-0.1210	2499170
6	4.8566	-0.0128	-149540	4130190	4.5007	9.3353	-0.1457	2811420
4	5.1231	0.0257	-150200	4315720	4.7438	9.7564	-0.1571	2907780
2	5.2358	0.0235	-155000	4464970	4.9288	9.9554	-0.1599	2990260
0	5.3284	0.0436	-154230	4532040	4.9877	10.0654	-0.1619	3026720
-2	5.2653	0.0403	-178660	4497190	4.9574	9.9248	-0.1763	2986360
-4	5.1956	0.0400	-172150	4397720	4.9174	9.7109	-0.1885	2934220
-6	5.0361	0.0748	-176180	4169610	4.7958	9.3189	-0.1859	2827200
-10	4.4592	0.1121	-173600	3662580	4.3991	8.2005	-0.1993	2558700
-14	3.6818	0.1217	-179750	3001390	3.8205	6.6409	-0.2137	2072320
-18	2.8468	0.1628	-201690	2174990	3.0776	4.9722	-0.2135	1545490
-22	1.7473	0.2081	-216010	998501	1.9217	3.0750	-0.2247	991161

Table A-9. Activity IV-A, Test 6, Experimental Configuration B, NW Unbalanced -4, Axial Measurements

	Detector Location and Name							
	SE	SE	NW	SW	NE	H-11	H-11	H-3
Inches from core center	Hf-658 primary (pico-amps)	Hf-658 background (pico-amps)	U-238 FC 4 (counts per minute)	U-235 FC 2252 (counts per minute)	Rh DN1 (pico-amps)	Hf-657 primary (pico-amps)	Hf-657 background (pico-amps)	U-235 FC 2253 (counts per minute)
30	0.1871	0.0094	0.0963	83477	0.2070	0.5907	-0.0158	262585
26	0.5474	-0.0069	0.5329	430109	0.6839	1.4738	-0.0244	666566
22	1.4511	-0.0094	1.2354	1076560	1.3660	2.9329	-0.0162	790417
18	2.5244	-0.0062	2.1233	1972360	2.3458	4.8729	-0.0247	1305990
14	3.5515	0.0017	3.0359	2887130	3.2311	6.6938	-0.0367	1865370
10	4.3856	0.0170	3.8024	3628270	4.0111	8.1445	-0.0603	2380850
6	4.9579	0.0606	4.3874	4188060	4.5733	9.0988	-0.0765	2707020
4	5.1704	0.0564	4.6448	4333760	4.8126	9.4896	-0.0790	2812360
2	5.2986	0.0774	4.8226	4469390	4.9288	9.6188	-0.0845	2868290
0	5.3931	0.0788	4.9637	4551020	5.0237	9.7485	-0.0960	2896990
-2	5.3566	0.0944	5.0054	4555010	4.9896	9.5949	-0.1023	2878140
-4	5.2612	0.1089	4.9796	4410650	4.9577	9.3721	-0.1153	2842410
-6	5.0218	0.1073	4.8339	4154710	4.7915	8.9170	-0.1172	2706270
-10	4.5533	0.1239	4.5697	3731150	4.4818	7.9767	-0.1396	2455380
-14	3.8256	0.1722	4.0357	3067080	3.8917	6.5426	-0.1471	2018490
-18	2.9225	0.1988	3.3413	2200700	3.1167	4.8540	-0.1548	1492890
-22	1.7846	0.2299	2.2841	1000550	1.9298	2.9738	-0.1574	955264

Table A-10. Activity III, Test 8, Experimental Configuration C, Axial Measurements

	Detector Location and Name					
	SE	NW	SW	NE	H-11	H-3
Inches from core center	Rh DN2 (pico-amps)	Rh DN3 (pico-amps)	Rh DN5 (pico-amps)	Rh DN1 (pico-amps)	Rh DN4 (pico-amps)	2253 FC (Counts per minute)
30	0.3186	0.2134	0.2916	0.1722	0.9077	272349
28	0.4752	0.3097	0.4654	0.2825	1.3341	451649
26	0.9786	0.6472	1.0600	0.6632	1.8524	694832
24	1.7427	1.1011	1.6184	1.0409	2.0948	790372
22	2.3447	1.4558	2.2668	1.4033	2.6497	825652
20	3.1212	1.9310	3.0313	1.8757	3.4450	1030450
18	3.9549	2.4461	3.8514	2.3582	4.3315	1331100
16	4.7418	2.9592	4.4630	2.8084	5.1516	1642240
14	5.5770	3.4858	5.4682	3.3112	6.0564	1932770
12	6.2689	3.9315	6.1329	3.6929	6.8384	2190110
10	6.8638	4.3005	6.7147	4.0471	7.5329	2425280
8	7.3707	4.6283	7.2039	4.3347	8.1156	2647820
6	7.8146	4.9387	7.6225	4.5915	8.5623	2762110
4	8.1944	5.1950	8.0187	4.8066	9.0033	2865270
2	8.4828	5.4217	8.2879	4.9514	9.2525	2960270
0	8.6446	5.5534	8.4474	5.0498	9.5278	2967040
-2	8.6063	5.5723	8.4279	5.0408	9.5932	2946630
-4	8.5624	5.5610	8.3476	5.0053	9.6354	2871660
-6	8.3463	5.4440	8.1356	4.8754	9.5547	2785080
-8	8.1864	5.3530	7.9372	4.7604	9.5366	2712910
-10	7.8475	5.1406	7.5721	4.5764	9.1874	2534500
-12	7.3887	4.8628	7.1129	4.3036	8.7909	2283370
-14	6.7930	4.5126	6.5307	3.9876	8.2853	2058520
-16	6.2114	4.1177	5.8841	3.5783	7.7055	1798510
-18	5.5383	3.7061	5.1576	3.1586	7.1230	1512090
-20	4.7657	3.1943	4.3425	2.6930	6.5216	1233440
-22	3.6989	2.5275	3.1440	2.0110	5.9291	974254

Table A-11. Activity III, Test 8, Experimental Configuration C, Power Linearity Measurements

	Detector Location and Name					
	SE	NW	SW	NE	H-11	H-3
Power (log N)	Rh DN2 (pico-amps)	Rh DN3 (pico-amps)	Rh DN5 (pico-amps)	Rh DN1 (pico-amps)	Rh DN4 (pico-amps)	2253 FC (counts per minute)
0.00065	-0.6678	-0.1353	-0.1338	-0.1404	-0.0754	110
0.02	-0.0041	-0.0282	0.0284	-0.0327	-0.0057	714
0.1	0.0083	-0.0185	-0.0195	-0.0007	0.0023	1848
1	0.0667	0.0081	0.0227	0.0195	0.0550	15932
10	0.5053	0.3122	0.4484	0.2836	0.5356	159262
50	2.4053	1.5463	2.3343	1.4101	2.6198	814244
100	4.8304	3.1085	4.6967	2.8329	5.2451	1629020
150	7.3086	4.7185	7.1101	4.2915	7.9895	2500620
180	8.6290	5.5662	8.4039	5.0546	9.4862	2983780

Table A-12. Activity IV, Test 9, Experimental Configuration C, Power Split Measurements

	Detector Location and Name					
	SE	NW	SW	NE	H-11	H-3
Estimated Power and Measured Data	Rh DN2 (pico-amps)	Rh DN3 (pico-amps)	Rh DN5 (pico-amps)	Rh DN1 (pico-amps)	Rh DN4 (pico-amps)	2253 FC (counts per minute)
Balanced Estimated Reactor Power (W)	57.27	39.75	56.71	40.53	55.74	55.74
Balanced Measured Data	8.6290	5.5662	8.4039	5.0546	9.4862	2983780
NW OSCC +4 Estimated Reactor Power (W)	56.88	40.92	56.32	40.14	55.74	55.74
NW OSCC +4 Measured Data	5.5417	6.1237	8.3951	5.0518	9.6732	3043990
NW OSCC -4 Estimated Reactor Power (W)	57.67	38.57	57.11	40.92	55.74	55.74
NW OSCC -4 Measured Data	8.6169	4.9082	8.3217	5.0109	9.3182	2939940